Axial Ligation Equilibria and Dynamics in a Redox Polyether Hybrid: An Fe Tetraphenylporphyrin Melt

Jeffrey W. Long[†] and Royce W. Murray*

Kenan Laboratories of Chemistry, University of North Carolina, Chapel Hill, North Carolina 27599-3290

Received February 12, 1998

Pyridine axial ligation is investigated in a molten Fe tetraphenylporphyrin fashioned by attaching oligomeric (MW 550) ethylene glycol chains at the *p*-phenyl ring positions ([Fe(T550PP)Cl]). Dissolution of $LiClO_4$ electrolyte renders the highly viscous, room-temperature melt (0.40 M in porphyrin sites) modestly ionically conductive, so that microelectrode voltammetry can be employed to follow axial pyridine ligation in a thin film of Fe porphyrin melt resting on the electrode assembly. Introduction of pyridine at the gas/melt interface produces distinctive changes in the microelectrode voltammetry, from which relative populations of chloride and pyridine-coordinated Fe(III) porphyrin can be measured and equilibrium constants for ligation of the Fe(III) and Fe(II) oxidation states estimated. Removal of the pyridine at the porphyrin melt/gas interface causes dissociation of the ligating pyridine in an overall process that has a time constant on the order of 5−10 min at 25 °C.

As recently described,[1] para-attachment of oligomeric (MW 550) ethylene glycol chains to the tetraphenylporphyrin macrocycle produces a material ([Fe(T550PP)Cl]) that in its undiluted form is 0.40 M in porphyrin sites, is a highly viscous, amorphous melt at room temperature, and is a good solvent for $LiClO_4$ electrolyte, which renders the melt modestly ionically conductive.

"Fe(T550PP)-Cl"

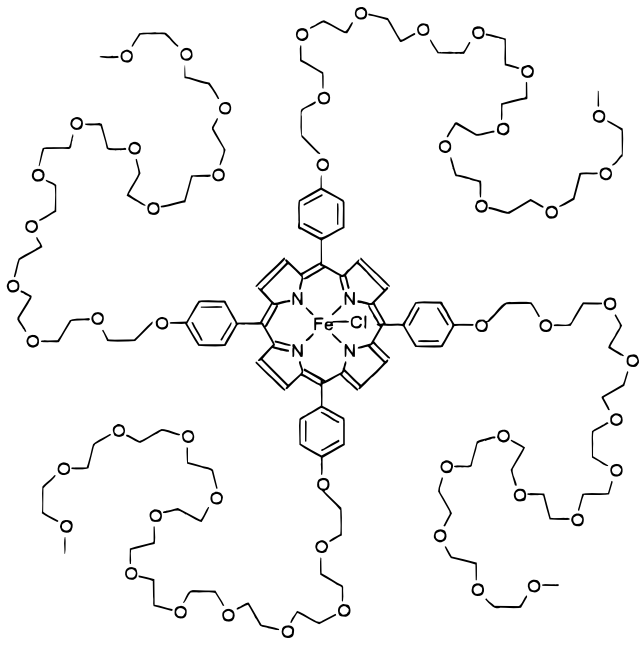

Microelectrode voltammetry of porphyrin melts showed[1] that the polyether-tailed porphyrins self-diffuse very slowly (ca. 3 × 10^{-12} cm^2/s) in their undiluted selves and that, in general, the porphyrin oxidation and reduction reactions occur by electron self-exchange transport through the mixed valent interfacial melt region, a process formally analogous to electrochemical reactions of redox polymers.[2,3] The homogeneous electron self-exchange rate constants for the Fe(III/II) and Fe(II/I) reactions were estimated[1] to be 1 × 10^4 and 4 × 10^4 M^{-1} s^{-1}, respectively.

The electrochemical reactions of dilute solutions of iron porphyrins have been extensively investigated,[4−9] including in particular the sensitivity of the Fe(III/II) reaction to the solvent medium and to the presence of axially coordinating ligands. Differences between the propensities of the Fe(III) and Fe(II) oxidation states for axial ligation cause shifts of the Fe(III/II) formal potential. Ligands such as chloride stabilize the Fe(III) state, shifting the formal potential to more negative values, while coordinating solvents such as dimethyl sulfoxide and dimethylformamide preferentially stabilize the Fe(II) state, shifting the Fe(III/II) reaction potential positively.[6]

A classic example of ligation is that of pyridine to Fe(III) tetraphenylporphyrin chloride, which for [Fe(TPP)Cl] has been studied in some detail.[5,8,9] The Fe(III) porphyrin can axially bind one (in coordinating solvents) or two (in noncoordinating solvents) pyridines, but only weakly in relation to the strong coordination to the Fe(II) state, which for pyridine is always diaxially coordinated.[6,9] The positive shift of the formal potential

[†] Present address: Naval Research Laboratory, Code 6170, Surface Chemistry, 4555 Overlook Ave., Washington, DC 20375-5342.

(1) Long, J.; Kim, I.; Murray, R. W. *J. Am. Chem. Soc.* **1997**, *119*, 11510.
(2) Sosnoff, C. S.; Sullivan, M.; Murray, R. W. *J. Phys. Chem.* **1994**, *98*, 13643.
(3) Murray, R. W., Ed. *Molecular Design of Electrode Surfaces*, in the series *Techniques of Chemistry*; John Wiley and Sons: New York, 1992.
(4) Kadish, K. M. In *Iron Porphyrins*; Lever, A. B. P., Gray, H. B., Eds.; Addison-Wesley: Reading, MA, 1983; pp 161−241.
(5) Constant, L. A.; Davis, D. G. *Anal. Chem.* **1975**, *47*, 2253.
(6) Bottomley, L. A.; Kadish, K. M. *Inorg. Chem.* **1981**, *20*, 1348.
(7) Kadish, K. M.; Morrison, M. M.; Constant, L. A.; Dickens, L.; Davis, D. G. *J. Am. Chem. Soc.* **1976**, *98*, 8387.
(8) Kadish, K. M.; Bottomley, L. A. *Inorg. Chem.* **1980**, *19*, 832.
(9) Kadish, K. M.; Bottomley, L. A.; Beroiz, D. *Inorg. Chem.* **1978**, *17*, 1124.

10.1021/ic980163c CCC: $18.00
Published on Web 12/10/1998

of the Fe(III/II) reaction that is provided by pyridine stabilization of the Fe(II) state is given by[4,8]

$$E^{\circ\prime}_{\mathrm{COMPLX}} - E^{\circ\prime}_{\mathrm{SOLVT}} = -0.059 \log\left[\frac{K_{\mathrm{FeIII}}}{K_{\mathrm{FeII}}}\right] - 0.059 \log[\mathrm{L}]^{p-q} \quad (1)$$

where $E^{\circ\prime}_{\mathrm{COMPLX}}$ and $E^{\circ\prime}_{\mathrm{SOLVT}}$ are formal potentials in the presence and absence (in the native solvent) of ligand L, respectively, K_{FeIII} and K_{FeII} are the stability constants of the L-ligated Fe(III) and Fe(II) states, respectively, [L] is the concentration of ligand, and p and q are the number of ligands coordinated to the Fe(III) and Fe(II) states, respectively. Information on the ligation stoichiometry and the relative values of K_{FeIII} and K_{FeII} can be obtained by measuring $E^{\circ\prime}_{\mathrm{COMPLX}} - E^{\circ\prime}_{\mathrm{SOLVT}}$ as a function of [L]. Determination of the individual stability constants requires additional information, such as the relative concentrations of pyridine- and chloride-ligated porphyrin.

This report extends iron tetraphenylporphyrin/pyridine ligation chemistry into the semisolid state, using the above [Fe(T550PP)Cl] melt material. Following a preliminary experiment[10] on a dilute polyether solution of [Fe(TPP)PF_6], we take advantage here of the low volatility of the [Fe(T550PP)Cl] melt to introduce and remove pyridine at the melt/gas interface of a thin film of [Fe(T550PP)Cl] resting on a microelectrode assembly. The appearance of the voltammetric signature of pyridine-ligated Fe(III) porphyrin and its dependence on the pyridine vapor pressure and on the removal of the pyridine bathing gas are used as a basis for estimating ligation stability constants and the dynamics of pyridine dissociation from the Fe(III) form.

Experimental Section

Chemicals, Microelectrodes, and Film Preparation. The attachment of monomethyl-terminated poly(ethylene glycol) (MW 550, av 12 repeat units) to free base tetra(*p*-hydroxyphenyl)porphyrin, and its subsequent metalation, has been described recently.[1] Thin films of the porphyrin product ([Fe(T550PP)Cl]) were cast from methanol solutions onto a polished, insulating platform on which are exposed the tips of 25 μm Pt (microdisk working electrode), 0.5 mm Ag (quasi-reference electrode, QRE), and 24 gauge Pt (counter electrode) wires. Evaporating the methanol under a stream of N_2, the coated microelectrode assembly was placed in a glass cell designed for exposure of the film to selected bathing gases.[11] The film was dried further under vacuum and at $\sim$ 70 °C for at least 24 h; this is important because residual solvents can strongly affect charge and mass transport rates. Film thicknesses were estimated to be 40 μm based on the mass of [Fe(T550PP)Cl] used to cast the films, which also contained either 0.4 or 1.2 M $LiClO_4$ (48:1 and 16:1 ether oxygen/Li, respectively) as supporting electrolyte.

The glass cell containing the microelectrode assembly was operated in a flow-through mode with individually controllable mass flow meters (Cole-Parmer). One meter fed dry N_2 to a swagelock tee joint mixer, while the other fed dry N_2 through a bubbler in a vial of pyridine liquid at room temperature and then to the mixer. A mineral oil exit bubbler excluded room air from the electrochemical cell, which for temperature control was placed in the oven of a Shimadzu GC-9A gas chromatograph. Some experiments were done in a plug flow mode, in which case the glass cell was placed in-line with the column of the gas chromatograph.

Electrochemical Instrumentation. Electrochemical measurements were performed using a locally built system consisting of a high sensitivity potentiostat controlled by an IBM-compatible 486-25 through a Datel 412 12-bit A/D board, with locally written software.

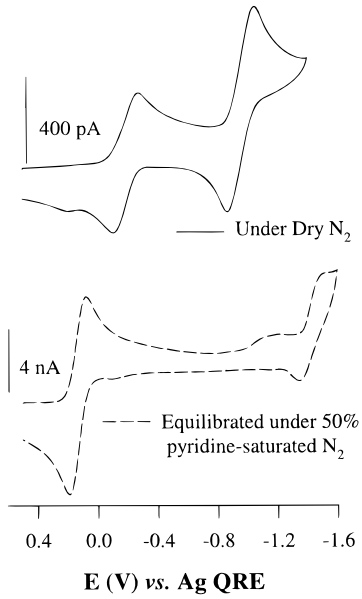

Figure 1. Cyclic voltammograms (100 mV/s) of [Fe(T550PP)Cl] melt containing 0.4 M $LiClO_4$ (48:1 ether O:Li ratio) at 25 °C. The more positive and negative waves represent Fe(III/II) and Fe(II/I) reactions. Upper: melt film under dry N_2. Lower: melt film equilibrated under flow of pyridine/N_2 at 50% pyridine saturation.

Results and Discussion

Effects of Ligation on Redox Potentials. Microelectrode voltammetry of a film of [Fe(T550PP)Cl] under dry N_2 (Figure 1, top) exhibits well-formed waves for the Fe(III/II) and Fe(II/I) reactions with formal potentials ($E^{\circ\prime}$, av of peak potentials) -0.19_5 V and -0.98 V, respectively, vs Ag QRE. The $\Delta E^{\circ\prime} =$ 0.78 V potential difference, as noted in our previous study,[1] suggests that the polyether chains attached to the porphyrin structure comprise a weakly coordinating "solvent" that should offer little competition to a strong ligand like pyridine, since this $\Delta E^{\circ\prime}$ is analogous to that of a dilute porphyrin solution in a noncoordinating solvent like CH_2Cl_2. The implication of this observation is that diaxial coordination of pyridine to the Fe(III) porphyrin is the likely case,[12] and indeed the data (vide infra) indicate that this is the case.

Exposure of the [Fe(T550PP)Cl] film to 50% saturated pyridine vapor for several minutes changes the voltammetry to that seen in Figure 1, bottom. The formal potential of the Fe(III/II) wave shifts positively by $+0.34$ V to $+0.14_5$ V vs Ag QRE and that for Fe(II/I) by -0.45 V negatively to -1.43 V vs Ag QRE. The effects of ligation on formal potentials for iron tetraphenylporphyrins are well-known; for example, $E^{\circ\prime}$ for the Fe(III/II) reaction in pyridine solvent shifts positively by 0.45 V and that for the Fe(II/I) reaction negatively by 0.44 V, as compared to CH_2Cl_2 solvent.[6] The porphyrin melt thus responds similarly to dilute porphyrin solutions, with respect to pyridine ligation, and the potential shifts of both reactions reflect stabilization of the Fe(II) state of the porphyrin by pyridine ligation.

Currents for the Fe(III/II) and Fe(II/I) reactions are enhanced by electron self-exchange transport in their mixed valent layers near the electrode−melt interface. In the N_2-bathed porphyrin melt, since electron self-exchange is faster for the Fe(II/I)

(10) Geng, L.; Reed, R. A.; Kim, M. H.; Wooster, T.; Oliver, B. N.; Egekeze, J.; Kennedy, R.; Jorgenson, J. W.; Parcher, J. F.; Murray, R. W. *J. Am. Chem. Soc.* **1989**, *111*, 1614.

(11) Long, J. W. Hybrid Redox Polyethers: Electrochemical Investigations in Molecular Melts of Metalloporphyrins and Metal Bipyridine Complexes. Ph.D. Thesis, University of NC, Chapel Hill, NC, l997.

(12) Satterlee, J. D.; La Mer, G. L.; Frye, J. S. *J. Am. Chem. Soc.* **1976**, *98*, 7275.13.

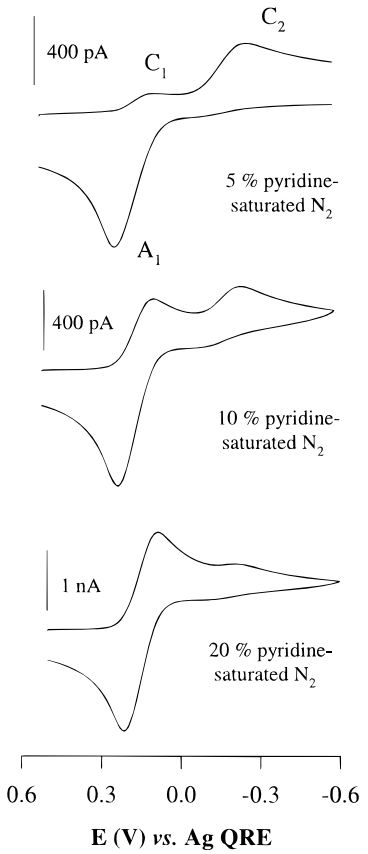

Figure 2. Fe(III/II) cyclic voltammograms (100 mV/s) for [Fe(T550PP)Cl] melt containing 1.2 M $LiClO_4$ (16:1 ether O:Li ratio) at 25 °C. Films have been equilibrated under gas flows of 5, 10, and 20% pyridine-saturated N_2 (at 25 °C).

reaction, its peak currents become larger (Figure 1, top). In the pyridine-bathed melt, the currents are more nearly equal, as shown in Figure 1, bottom, indicating that the Fe(III/II) and Fe(II/I) electron-hopping rates are in this case roughly the same in the pyridine-coordinated Fe porphyrin melt.

Further experiments presented here are confined to results for the Fe(III/II) reaction.

Effects of Pyridine Bath Concentration on Voltammetry. The quantity of pyridine partitioning into the [Fe(T550PP)Cl] melt phase, and the resulting Fe(III/II) voltammetry, varies with the composition of the pyridine−N_2 gas mixture bathing the electrochemical cell. Figure 2 shows room-temperature voltammetry for melt films that have been equilibrated under 5, 10, and 20% pyridine-saturated N_2 flows. Two reduction peaks (labeled C_1 and C_2) are seen on the negative potential scan, and a single oxidation peak (A_1, which is a partner of C_1) is observed on the subsequent positive-going scan. In more concentrated pyridine vapor baths, peak C_1 increases at the expense of peak C_2, while the oxidation peak A_1 remains the same size, *relative* to the reduction peaks.

The Figure 2 voltammograms can be understood in the context of a reaction scheme (Figure 3) that parallels the one previously proposed[8] for dilute solutions of [Fe(TPP)Cl] in weakly coordinating solvents. At small pyridine concentrations, the equilibrium constant K_{FeIII} governs the proportion of uncoordinated vs pyridine-coordinated forms of the Fe(III) porphyrin. Comparing peak potentials in Figures 1 and 2, peak C_2 must arise from the reduction of [Fe^{III}(T550PP)Cl], and peaks C_1 and A_1, respectively, to the reduction and subsequent oxidation of a pyridine-coordinated form of the porphyrin (which, anticipating a result below, we label [Fe^{III}(T550PP)-

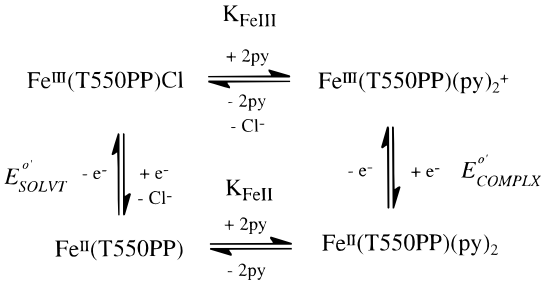

Figure 3. Reaction scheme for electron transfers and pyridine ligation of [Fe(T550PP)Cl].

Table 1. Dependence of Redox Potentials and Diffusion Coefficients on Pyridine Vapor Composition

% pyridine saturation in N_2 flow	E°_{COMPLX} (V vs Ag QRE)[a]	D_{APP} (cm^2/s)[b]
5	+0.13	6.1×10^{-10}
10	+0.15	4.2×10^{-9}
20	+0.15	2.0×10^{-8}
30	+0.15	5.3×10^{-8}
44	+0.13	1.2×10^{-7}
50	$+0.10_5$	1.5×10^{-7}
63	+0.12	2.9×10^{-7}
73	+0.13	5.7×10^{-7}

[a] Determined from $\{E_{PEAK,CATHODIC} - E_{PEAK,ANODIC}\}/2$ from the voltammetric wave (C_1, A_1) for the Fe(III/II) couple of pyridine-ligated porphyrin. [b] Determined from the anodic peak current (wave A_1) for the Fe(III/II) couple of the pyridine-ligated porphyrin, using the Randles-Sevcik equation.[24]

$(py)_2]^+$). The fact that peak C_2 lacks an oxidative counterpart means that, following reduction of [Fe^{III}(T550PP)Cl], nearly all of the product Fe(II) porphyrin undergoes rapid ligation by pyridine that is not reversed on the time scale of the positive potential scan (as has been seen previously in solutions of [Fe(TPP)Cl]).[5]

The relative concentrations of complexed and uncomplexed Fe(III) porphyrin that exist at equilibrium in a melt film bathed in pyridine vapor can be estimated from ratios of wave C_1 and C_2 peak currents taken at potential scan rates sufficiently fast ($\geq$100 mV/s)[13] that the equilibrium between complexed and uncomplexed Fe(III) porphyrin does not significantly shift on the time scale of the measurement.[5] These ratios give the percent of pyridine-complexed Fe(III) porphyrin as 15, 65, and 95%, in 5, 10, and 20%, respectively, pyridine-saturated N_2 bathing vapor. At higher (i.e., 50%) pyridine bathing concentration, the equilibrium has been shifted entirely toward the pyridine-coordinated Fe(III) porphyrin, as shown in Figure 1, bottom.

According to eq 1, any change in ligation stoichiometry (i.e., whether the Fe(III) porphyrin is singly or diaxially pyridine-coordinated) can be determined from the dependence of $E^{\circ\prime}_{COMPLX}$ on pyridine vapor concentration. Table 1 gives results for pyridine vapor composition varying from 5 to 73% pyridine-saturated N_2. There is no discernible trend within the somewhat scattered data for $E^{\circ\prime}_{COMPLX}$, within the uncertainties associated with a Ag quasi-reference electrode. Remembering that the Fe(II) state prefers[6,9] to be diaxially coordinated and assuming those kinetics to be rapid (the Fe(III) kinetics are slow but the

(13) Voltammograms were recorded at potential scan rates of 50, 100, 150, 200, and 250 mV/s in each case. Within this range of scan rates, the peak current ratio C_1/C_2 was constant, indicating no significant perturbation of the axial ligation equilibrium. For example values of C_1/C_2 for the case of the film exposed to 10% pyridine-saturated N_2 were 1.7, 1.8, 1.8, 1.8, and 1.8 at the above potential scan rates, respectively. A similar result was obtained for the cases of 5 and 20% pyridine-saturated N_2.

Table 2. Determination of Equilibrium Constants for Pyridine Ligation of [Fe(III)porphyrin]

% py sat'd in N_2	$[py]_{GAS}$ (M)[a]	$[py]_{FILM,TOTAL}$ (M)[b]	$[py]_{FILM,FREE}$ (M)[c]	$[Fe^{III}(py)_2]/[Fe^{III}Cl]$[d]	K_{FeIII} (M^{-2})[e]
5	5.4×10^{-5}	0.64	0.54	0.15	0.6
10	1.1×10^{-4}	1.28	0.77	1.8	3.1
20	2.1×10^{-4}	2.56	1.80	17	5.2

[a] Based on a vapor pressure of 19.6 Torr for 100% saturated pyridine vapor at 25 °C. [b] Total concentration of pyridine in the film, based on $K_{PART} = 1.2 \times 10^4$. (See ref 14) [c] Concentration of uncoordinated pyridine in the film at equilibrium, based on ligation of two pyridines to the Fe(III) porphyrin, a total porphyrin concentration of 0.40 M, and taking the fraction of bis-coordinated pyridine from the ratio of voltammetric peak currents of waves C_1 and C_2. [d] Determined from the ratio of voltammetric peak currents of waves C_1 and C_2, which did not vary with the potential scan rate (ref 13). [e] Calculated using eq 2.

ligation equilibrium is preestablished), the apparent lack of dependence of $E^{\circ\prime}_{COMPLX}$ on pyridine vapor concentration means that the Fe(III) form must also be diaxially coordinated.

Further analysis of the porphyrin melt phase ligation requires evaluation of the pyridine gas/melt partition equilibrium constant. This measurement was accomplished with a gas chromatography column in which a film of [Fe(T550PP)Cl] serves as the stationary phase. Measuring the retention time for pyridine passing through such a column yields the equilibrium constant for pyridine partitioning into the melt phase: $K_{PART} = [py]_{FILM,TOTAL}/[py]_{GAS}$. Pyridine has a rather high boiling temperature, and its low volatility precluded reliable measurements below 60 °C, so partition data taken at temperatures from 60 to 110 °C were extrapolated[14] to 25 °C. K_{PART} was, thereby, estimated at 25 °C as 1.2×10^4 under the conditions of Figures 1 and 2, from which the *total* concentrations of pyridine partitioned into the [Fe(T550PP)Cl] melt at 25 °C were calculated and are given in Table 2 as $[py]_{FILM,TOTAL}$.

Using the partition constant results, the stability constant K_{FeIII} in the melt can be calculated according to

$$K_{FeIII} = \frac{\{[Fe^{III}(T550PP)(py)_2]^+[Cl]^-\}}{[Fe^{III}(T550PP)Cl][py]^2_{FILM,FREE}} \qquad (2)$$

where the concentration $\{[Fe^{III}(T550PP)(py)_2]^+[Cl]^-\}$ assumes[16] that the chloride remains associated with the diaxially coordinated porphyrin as an ion pair (following prior work[17]), and the equilibrium concentration of pyridine residing in the polyether part of the melt phase, $[py]_{FILM,FREE}$, is $[py]_{FILM,\ TOTAL} - 2\{[Fe^{III}(T550PP)(py)_2]^+[Cl]^-\}$. The total[1] porphyrin concentration is 0.40 M, and the concentration ratio $\{[Fe^{III}(T550PP)(py)_2]^+[Cl]^-\}/[Fe^{III}(T550PP)Cl]$ of coordinated and noncoordinated Fe(III) porphyrin can be determined from the ratio of the voltammetric peak currents C_1 (coordinated) and C_2 (uncoordinated). These ratios and resulting values for K_{FeIII} are given in Table 2.

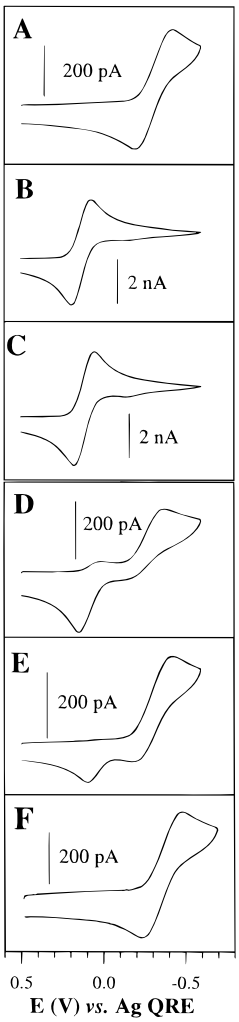

Figure 4. Voltammograms (100 mV/s) for the Fe(III/II) redox couple of [Fe(T550PP)Cl] melt containing 1.2 M $LiClO_4$ (16:1 ether O:Li ratio) at 25 °C: (A) initial, under dry N_2 flow; (B) after 4 min exposure to 50% pyridine-saturated N_2; (C) after 20 min as in (B); (D,E,F) 20 min, 3 h, 20 h after switching bathing gas to dry N_2.

The derived results (Table 2) for K_{FeIII} vary by ca. 8-fold over the range of bathing pyridine concentrations used. The source of this variation is unclear. It is not provoked by assuming ion pairing of $[Fe^{III}(T550PP)(py)_2]^+$ and chloride; an analysis assuming[16] chloride dissociation leads to much wider variation in K_{FeIII}. A possible concentration-dependent error is that the partition isotherm might be nonlinear; K_{PART} was chromatographically determined under conditions of very dilute pyridine vapor concentrations, whereas those in Table 2 are much larger.

On the basis of the above discussion, the lower pyridine concentration would be expected to give the more reliable result for the K_{FeIII} stability constant (0.6). Based on this value, the equilibrium constant for Fe(II) ligation, K_{FeII}, calculated from eq 1 is 2×10^5. These two equilibrium constants are similar to published values for dilute solutions of [Fe(TPP)Cl], where $K_{FeIII} = 0.5$ (in $CHCl_3$) and $K_{FeII} = 4 \times 10^5$ (in DMF).[8,9,17] While the uncertainities are acknowledged, these equilibrium data are the first available for axial coordination in molten metalloporphyrins.

Effects of Pyridine on Voltammetric Currents. The general magnitudes of peak currents seen in voltammetry (Figures 1, 2, 4) of the Fe porphyrin melt vary with the concentration of

(14) The extrapolation was done with a plot of log K_{PART} vs $1/T$ for data taken between 60 and 110 °C, which was linear. Partitioning at elevated temperatures is shown[15] to be accompanied by porphyrin ligation by the appearance of wave C_1; K_{PART} thereby reflects a total of free and Fe(III)-coordinated pyridine in the melt phase.

(15) Long, J. W.; Murray R. W. *Anal. Chem.* **1998**, *70*, 3355.

(16) Assuming chloride to be dissociated leads to values of $K_{FeIII} = 0.03$, 0.8, and 2 for 5, 10, and 20% saturated pyridine vapor, respectively. These results vary more widely than those in Table 2. It was not possible to explore the effect of adding chloride to the porphyrin melt. Melts containing only LiCl as electrolyte were too resistive to allow voltammetric measurements. The voltammetry was unchanged by adding LiCl to the $LiClO_4$ electrolyte, but LiCl had limited solubility in that case.

(17) Walker, F. A.; Lo, M. W.; Ree, M. T. *J. Am. Chem. Soc.* **1976**, *98*, 5552.

pyridine bathing vapor. Such variations might relate to changes in the rates of electron self-exchange transport as the porphyrin coordination state changes. However, judging from previous experience with dilute solutions of redox species in polyethers[10,18−21] and with redox polyether hybrid melts,[22,23] the current changes are more plausibly associated with diffusion-plasticization. The previous observations have shown that dissolution of small molecules in polyether polymer electrolytes substantially increases mass transport rates in the polymer; ionic conductivities and viscosities are similarly changed. Alcohols, nitriles, and pyridines are potent diffusion-plasticizing small molecules.

The plasticization current enhancement effects can be expressed through apparent diffusion coefficients (D_{APP}), which are calculated by applying the Randles−Sevcik equation[24] to the peak currents for the oxidation wave A_1. Results are given in Table 1. The D_{APP} values represent[1] some combination of physical and electron-hopping diffusivity and change by 10^3-fold over the range of investigated pyridine bathing concentrations. The changes in D_{APP} are incidental, we believe, to the other phenomena described in this paper, except for the process of pyridine de-ligation, discussed below.

Dynamics of Pyridine Entry and Exit from [Fe(T550PP)Cl] Melt Film. The melt/gas interface that allows facile introduction of volatile ligands into the porphyrin melt also allows their removal by replacing the bathing medium with dry N_2. This section considers the dynamics of such processes.

The dynamics of pyridine addition to and removal from the melt films are plausibly related to (a) pyridine partitioning between the bathing gas and the melt film and (b) the kinetics of pyridine−Fe axial coordination, which in turn depend on (c) the Fe oxidation state. The partitioning process depends on film thickness and pyridine mass transport rates. The latter, owing to its diffusion-plasticization effect (vide infra), will change in a complex manner over the course of partition equilibration.

Figure 4 shows a sequence of voltammograms for exposure of a melt film, initially under dry N_2, to a high concentration (50% saturated) of pyridine vapor and then back to dry N_2. A comparison of parts A and B of Figure 4 shows that, upon exposure to pyridine vapor, the Fe(III) porphyrin quickly becomes completely ligated, since little further voltammetric change occurs after a longer exposure period (Figure 4C). Upon switching the bathing gas back to dry N_2, after 20 min, reduction peak C_2 has increased at the expense of C_1 (Figure 4D), as pyridine partitions out of the polyether "solvent" and pyridine dissociates from the Fe(III) porphyrin, leaving only 15% of pyridine-coordinated Fe(III) porphyrin. After 3 h of exposure to dry N_2 (Figure 4E), peak C_1 has vanished; that is, no measurable equilibrium amount of $[Fe^{III}(T550PP)(py)_2]^+$ remains in the film. After 20 h under dry N_2, the voltammetry (Figure 4F) has at last quantitatively reverted to that originally observed (Figure 4A).

Under most voltammetric conditions of pyridine vapor exposure, sufficient ligand has partioned into the film that only peak A_1 (pyridine-complexed Fe(II) porphyrin) appears during the positive potential scan. Observing peak A_1 in experiments such as that in Figure 4, but at more frequent intervals, allowed following the time course of diffusion-plasticization, and thus of the main part of the pyridine-partitioning (which causes the plasticization). Voltammograms taken at 1 min intervals following exposure of a dry film (i.e., Figure 4A) to 50% saturated pyridine vapor show that currents for peak A_1 rise to a constant value within 5 min (i.e., Figure 4B,C), with a half-time of about 1 min. Thus, after only 1 min, sufficient pyridine has entered the film (>0.8 M) that the voltammogram exhibits only peak A_1 (i.e., oxidation of $[Fe^{II}(T550PP)(py)_2]$), and no peak for A_2. Upon switching the bathing gas to dry N_2, the peak current A_1 decreases (with a half-time of again about 1 min) and within ca. 5 min attains a value only ca. 5% of its previous 50%-saturated pyridine value. The voltammogram after 5 min is similar to Figure 4D peak current A_1, then decreases, quite slowly, to zero over a 6 h period; Figure 4E represents roughly the midpoint of this slow change. The short-time observations show that the large changes in peak A_1 currents are caused by the onset and disappearance of diffusion-plasticization effected by partitioned pyridine and that the plasticization-based changes *during in- and out-partioning are similar and are mainly over after about 5 min.*

On the other hand, the long-time observations indicate a prolonged residence of substantial residues of pyridine in the film, insufficient to induce diffusion-plasticization but still sufficient for coordination to the porphyrin. This persistent population is signaled by the relative sizes of currents for peak A_1 vs peaks C_1 and C_2. Figure 4D shows that after 20 min of dry N_2 exposure, A_1 is nearly as large as peaks C_1 and C_2 combined, meaning that the residual pyridine concentration is > 0.4 M. The presence of oxidation peak A_1 in Figure 4E shows that even after 3 h of dry N_2 exposure enough pyridine remains to capture a portion of the Fe(II) porphyrin produced in peak C_2 to become reoxidized as $[Fe^{II}(T550PP)(py)_2]$. The residual pyridine may have significance for the process of Fe(III) porphyrin de-ligation, discussed next.

Consideration of the Fe(III) axial ligation kinetics can be based on measuring the ligated Fe(III) porphyrin $[Fe^{III}(T550PP)(py)_2]^+$ concentration from the relative sizes of waves C_1 and C_2 as done above. If the rates of axial ligation and de-ligation are both rapid, then the time courses of changes in $[Fe^{III}(T550PP)(py)_2]^+$ concentration upon successive pyridine vapor and dry N_2 exposures should be similar to one another. However, they are not, as shown by results for $[Fe^{III}(T550PP)(py)_2]^+$ concentration in Figure 5. When a dry [Fe(T550PP)Cl] melt film is exposed to a large concentration (50% saturated) of pyridine vapor (●), the Fe(III) state becomes completely ligated (i.e., the wave C_1 grows to its full size and C_2 disappears) by the time the first voltammogram is recorded, at 1 min. In contrast, upon subsequent exposure to a dry N_2 flow (○), the $[Fe^{III}(T550PP)(py)_2]^+$ concentration decreases slowly, apparently much more so than the rate of removal (vide infra) of most of the pyridine in the film suggests. The latter result indicates that *under these experimental conditions the process of de-ligation of the Fe(III) porphyrin in its melt occurs with a 5−10 min half-life.*

Supporting evidence for a measurably slow de-ligation of pyridine from $[Fe^{III}(T550PP)(py)_2]^+$ is provided by comparison of two voltammetric experiments (Figure 6) in which the degree of diffusion-plasticization caused by partitioned pyridine is nearly the same, as gauged by the size of A_1 peak currents. In one case (solid line), the [Fe(T550PP)Cl] melt was equilibrated

(18) Pyati, R.; Murray, R. W. *J. Am. Chem. Soc.* **1996**, *118*, 1743.
(19) Haas, O.; Velázquez, C. S.; Porat, Z.; Murray, R. W. *J. Phys. Chem.* **1995**, *99*, 15279.
(20) Barbour, C. J.; Parcher, J. F.; Murray, R. W. *Anal. Chem.* **1991**, *63*, 604.
(21) Geng, L.; Longmire, M.; Reed, R. A.; Parcher, J. F.; Barbour, C. J.; Murray, R. W. *Chem. Mater.* **1989**, *1*, 58.
(22) Velázquez, C. S.; Hutchison, J. E.; Murray, R. W. *J. Am. Chem. Soc.* **1993**, *115*, 7896.
(23) Pinkerton, M.; Le Mest, I.; Zhang, H.; Watanabe, M.; Murray, R. W. *J. Am. Chem. Soc.* **1990**, *112*, 3730.
(24) $I_{peak} = (2.69 \times 10^5)n^{3/2}ACD^{1/2}\nu^{1/2}$.

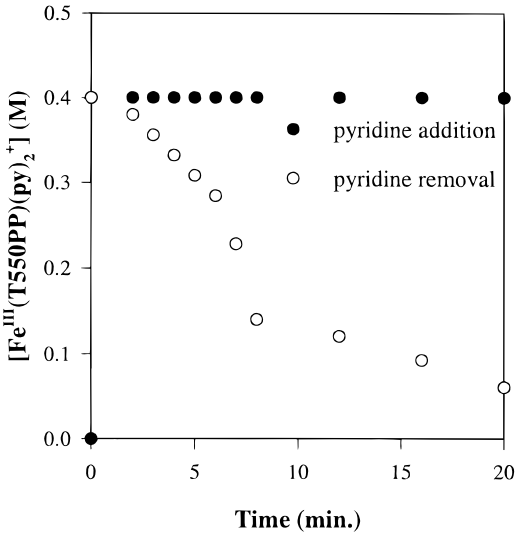

Figure 5. Concentration of pyridine-coordinated porphyrin, $[Fe^{III}(T550PP)(py)_2]^+$, as a function of time following exposure of dry [Fe(T550PP)Cl] melt containing 1.2 M $LiClO_4$ to pyridine vapor (50% saturation in N_2) (●) and subsequently to dry N_2 (○). The gas flow rate is 62 mL/min. Concentration was calculated based on peak currents for waves C_1 and C_2 and a total porphyrin concentration of 0.4 M.

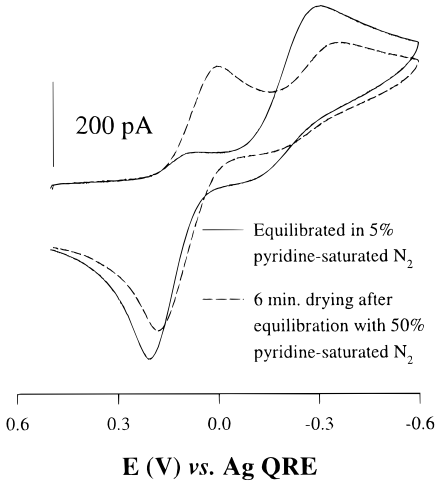

Figure 6. Voltammetry (100 mV/s) for [Fe(T550PP)Cl] films with similar pyridine contents as judged from nearly identical A_1 currents: after equilibration under a stream of 5% pyridine-saturated N_2 (solid line) and after initial equilibration under 50% pyridine-saturated N_2, followed by 6 min under dry N_2 stream (62 mL/min, dashed line).

under 5% pyridine-saturated N_2. In the second case (dashed line), the same film was equilibrated under 50% pyridine-saturated N_2 and subsequently dried for 6 min under a flow of N_2. Peak A_1 is nearly identical in the two experiments, so the diffusion-plasticization effect should be similar in the two experiments. However, in the first case (—), the relative sizes of peaks C_1 and C_2 show that only 15% of the Fe(III) porphyrin is complexed, whereas in the case (- - -) where pyridine is being removed, 71% remains complexed. As the first case represents an equilibrated condition, the excess of pyridine-complexed porphyrin in the second experiment must be ascribed to a slow de-ligation process.

The relative slowness of Fe(III) porphyrin de-ligation may be connected as much to the slowness of out-partitioning of the pyridine ligand upon exposure of the melt film to a flowing bath of dry N_2 as to the intrinsic kinetics of Fe(III) de-ligation. The discussion above showed that a substantial residue of pyridine remains even after enough of it has out-partitioned to

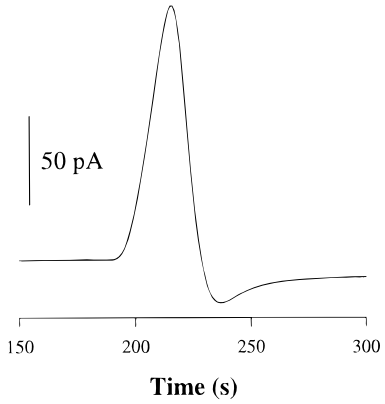

Figure 7. Amperometric signal for [Fe(T550PP)Cl] film containing 0.4 M $LiClO_4$ transiently exposed to a vapor plug of pyridine (1.0 μL injection) at 80 °C eluting from a 2.0 m poly(dimethylsiloxane) column. The microdisk electrode is at 0.0 V vs Ag QRE.

abate the diffusion-plasticization enhancement of transport rates in the film. A possible reason is that the loss of diffusion-plasticization will occur beginning at the film/gas interface, generating a transport barrier (i.e., slowed pyridine diffusion) there that subsequently traps the remaining pyridine in the lower portion of the film (where the electrode resides) for prolonged periods. That is, a nonuniform loss of diffusion-plasticization may provide a mechanism for retaining enough pyridine in the film to slow the rate of the overall process of Fe(III) porphyrin de-ligation.[25] The possibility of actual rate control by the de-ligation step itself is rendered inconclusive by this complication.

Transient Exposure of Porphyrin Melt Film to Pyridine. One aspect of the ligation chemistry of [Fe(T550PP)Cl] melt films is the possibility of producing selective electrochemical gas detectors. For example, in a gas chromatography context, a microelectrode detector coated with [Fe(T550PP)Cl] could be housed within the oven of a chromatograph. A study of such an "ECGC" detector is described elsewhere.[15] Results from transient exposures of [Fe(T550PP)Cl] films to ligand vapors in that study provided further insights into slow pyridine de-ligation from the porphyrin melt film, but in this case from the $[Fe^{II}(T550PP)(py)_2]$ form. Figure 7 shows the result of exposure of the porphyrin film to a plug of very dilute pyridine vapor exiting from a GC column and passing over the film at 80 °C. The microelectrode potential is held at 0 V vs Ag QRE, which, according to Figure 4A,B, is insufficiently negative to reduce $[Fe^{III}(T550PP)Cl]$ but is sufficiently negative to reduce the ligated form, $[Fe^{III}(T550PP)(py)_2]^+$. The current recorded while the pyridine vapor plug passes by is thus expected to report the time course over which the $[Fe^{III}(T550PP)(py)_2]^+$ concentration changes; it rises on the leading edge of the pyridine vapor plug as in-partitioning occurs and falls with the reverse process.

A rise-then-fall of $[Fe^{III}(T550PP)(py)_2]^+$ reduction current is indeed observed in Figure 7, and its profile correlates quantitatively with the response of the flame ionization detector of the chromatograph to the pyridine vapor plug. However, the trailing edge of the chromatographic peak also displays a prolonged dip of current *below baseline*; that is, an *oxidation* current is measured. From the preceding, and in view of the scheme in Figure 3, the oxidation current must arise from

(25) A reviewer suggested, based on earlier literature,[26] that autoreduction of Fe(III) porphyrin by pyridine might lead to its retention in the film. The earlier report, however, involves a rather minor effect and very different conditions, and was later disputed.[5]

(26) Epstein, L. M.; Straub, D. K.; Maricondi, C. *Inorg. Chem.* **1967**, *6*, 1720.

oxidation of the diffusion layer of reduced porphyrin, [Fe^{II}-(T550PP)$(py)_2$], formed around the microelectrode during the passage of the pyridine vapor plug, as it dissociates pyridine ligand to form [Fe^{II}(T550PP)], which is oxidizable at 0 V. The reduced complex [Fe^{II}(T550PP)$(py)_2$] tenaciously retains the coordinated pyridine, so its de-ligation is slow. The time constant of the latter process in Figure 7 is much faster than that in Figures 5 and 6, which were at room temperature. The Figure 7 experiment was conducted at 80 °C, where de-ligation rates should be faster and where the in-partitioned pyridine concentration is much smaller and diffusion-plasticization is unimportant.

Acknowledgment. This research was supported in part by grants from the Department of Energy and the National Science Foundation.

IC980163C